



# Influence of Light on Particulate Organic Matter Utilization by Attached and Free-Living Marine Bacteria

Laura Gómez-Consarnau<sup>1,2\*</sup>, David M. Needham<sup>2</sup>, Peter K. Weber<sup>3</sup>, Jed A. Fuhrman<sup>2</sup> and Xavier Mayali<sup>3\*</sup>

<sup>1</sup> Departamento de Oceanografía Biológica, Centro de Investigación Científica y de Educación Superior de Ensenada (CICESE), Ensenada, Mexico, <sup>2</sup> Department of Biological Sciences, University of Southern California, Los Angeles, CA, United States, <sup>3</sup> Lawrence Livermore National Laboratory, Livermore, CA, United States

## OPEN ACCESS

### Edited by:

Peta L. Clode,  
The University of Western Australia,  
Australia

### Reviewed by:

Connie Lovejoy,  
Laval University, Canada  
Holly M. Simon,  
Oregon Health & Science University,  
United States

### \*Correspondence:

Laura Gómez-Consarnau  
consarnau@cicese.mx;  
gomezcon@usc.edu  
Xavier Mayali  
mayali1@llnl.gov

### Specialty section:

This article was submitted to  
Microbial Physiology and Metabolism,  
a section of the journal  
Frontiers in Microbiology

**Received:** 31 January 2019

**Accepted:** 13 May 2019

**Published:** 04 June 2019

### Citation:

Gómez-Consarnau L,  
Needham DM, Weber PK,  
Fuhrman JA and Mayali X (2019)  
Influence of Light on Particulate  
Organic Matter Utilization by Attached  
and Free-Living Marine Bacteria.  
*Front. Microbiol.* 10:1204.  
doi: 10.3389/fmicb.2019.01204

Light plays a central role on primary productivity of aquatic systems. Yet, its potential impact on the degradation of photosynthetically produced biomass is not well understood. We investigated the patterns of light-induced particle breakdown and bacterial assimilation of detrital C and N using <sup>13</sup>C and <sup>15</sup>N labeled freeze-thawed diatom cells incubated in laboratory microcosms with a marine microbial community freshly collected from the Pacific Ocean. Particles incubated in the dark resulted in increased bacterial counts and dissolved organic carbon concentrations compared to those incubated in the light. Light also influenced the attached and free-living microbial community structure as detected by 16S rRNA gene amplicon sequencing. For example, Sphingobacteriia were enriched on dark-incubated particles and taxa from the family Flavobacteriaceae and the genus *Pseudoalteromonas* were numerically enriched on particles in the light. Isotope incorporation analysis by phylogenetic microarray and NanoSIMS (a method called Chip-SIP) identified free-living and attached microbial taxa able to incorporate N and C from the particles. Some taxa, including members of the Flavobacteriaceae and Cryomorphaceae, exhibited increased isotope incorporation in the light, suggesting the use of photoheterotrophic metabolisms. In contrast, some members of Oceanospirillales and Rhodospirillales showed decreased isotope incorporation in the light, suggesting that their heterotrophic metabolism, particularly when occurring on particles, might increase at night or may be inhibited by sunlight. These results show that light influences particle degradation and C and N incorporation by attached bacteria, suggesting that the transfer between particulate and free-living phases are likely affected by external factors that change with the light regime, such as time of day, water column depth and season.

**Keywords:** photoheterotrophy, proteorhodopsin, aerobic anoxygenic phototrophy, microbial loop, free-living bacterioplankton, particle-attached bacterioplankton

## INTRODUCTION

Photoheterotrophy is a major biogeochemical process in surface waters. Although this dogma is now recognized across the aquatic microbiology field (Béjà et al., 2000; Kolber et al., 2000), until the year 2000 all marine heterotrophic bacteria were classified as strict organic matter decomposers. Two major light energy transducing mechanisms are now identified in surface bacterioplankton: proteorhodopsin (PR) photoheterotrophy and aerobic anoxygenic phototrophy (AAP). PRs are the most abundant and widespread of the two. Notably, they are present and highly expressed in many bacteria including those from the SAR11 clade (Giovannoni et al., 2005; Gifford et al., 2013; Ottesen et al., 2013, 2014) and most studies suggest that they are ubiquitous in nutrient-depleted waters (e.g., the Eastern Mediterranean Sea; Dubinsky et al., 2017). However, PRs have also been identified in bacteria adapted to grow on organic matter-rich particles such as the Flavobacteria (Gómez-Consarnau et al., 2007; Gonzalez et al., 2008; Riedel et al., 2013; Maresca et al., 2018). These nutrient-rich particle-associated microenvironments also seem to be preferred by some AAP bacteria, such as the Rhodobacteraceae commonly found after seasonal phytoplankton blooms (e.g., Allers et al., 2007) and during outdoor cultivation of microalgae (Geng et al., 2016). One unanswered question is whether light energy from PR photoheterotrophy and AAP can be used by those microorganisms to optimize their resource utilization for the degradation of complex particulate organic matter.

Previous studies carried out in free-living communities strongly suggest that photoheterotrophy plays a role in dissolved organic matter (DOM) degradation. A study in the North Pacific subtropical gyre at station ALOHA reported bacterial production rates 48–92% higher in the light compared to the dark using radiolabeled leucine incorporation (Church et al., 2004). While the microbial groups responsible for the observed light-enhanced uptake rates were not identified, the authors attributed this observation to possible *Synechococcus* amino acid uptake. Similarly, Michelou et al. (2007) showed that light stimulated both amino acid assimilation and bacterial production; in this case the effect did not correlate with cyanobacterial abundances nor with the growth of photoheterotrophic AAP. Other field studies have reported that both *Prochlorococcus* and low nucleic acid (LNA) bacteria (often dominated by the PR-containing SAR11 bacterial clade) show a significant increase in amino acids uptake in the light compared to the dark (Mary et al., 2008; Gómez-Pereira et al., 2013; Evans et al., 2015). These data indicate that photoheterotrophy can help support dissolved organic matter processing. However, whether or not light can also stimulate the uptake or degradation of particulate organic matter is currently unknown.

Although no studies have thus far examined the role of photoheterotrophy in the degradation of algal-derived particles, there is ample literature about the role of particle degradation in ocean carbon cycling (reviewed by Simon et al., 2002). These studies have determined that particle-attached microbes are (i) phylogenetically diverse, often (but not always) dominated by Bacteroidetes known to degrade polysaccharides, (ii) exhibit high

solubilization rates, and (iii) may release labile substrates into the surrounding water (Azam and Long, 2001). Understanding the interplay between free-living and particle-attached bacteria is key to further constrain the role of particles in elemental cycling. This question has been explored previously in dark incubations of live diatoms in laboratory rolling tanks (Passow et al., 2003), showing initial increases of biomass in particulate aggregates, further suggesting that the attachment of initially free-living bacteria may bring carbon from the free-living to the particulate phase. Bacteria have also been shown to rapidly attach and detach from particles but become irreversibly attached after some period of time (Kjørboe et al., 2003). Particle-attached bacteria exhibit higher bacterial protein production and higher protease activity per cell than when free-living (Grossart et al., 2007). In one example, polysaccharide-degrading bacterial strains could grow on laminarin (one of the most common carbohydrates in the sea) and released glucose and larger glucans in this process (Alderkamp et al., 2007). Yet, no previous reports have documented particulate organic matter (POM) being released and subsequently incorporated by free-living bacteria; furthermore, the role of light and photoheterotrophy in the process of particulate breakdown remains uncharacterized.

In the current study, we address some of these unanswered questions using laboratory incubations of a microbial community that started as primarily free-living in the presence of stable isotope labeled phytodetrital particles. We aimed to test the hypothesis that photoheterotrophy enhances the transport of organic compounds from particles into bacterial cells, which would be consistent with light promoting the degradation of POM. This process is expected to be more significant in taxa known to be particle-attached photoheterotrophs such as members of Flavobacteria and Rhodobacterales. We carried out laboratory incubation experiments using freshly collected free-living marine bacterial communities with diatom-derived particles to link the activity of both attached and free-living bacteria to the incorporation of particulate material. Dead, isotopically labeled phytoplankton cells were mixed with marine microbial communities in rolling bottles to increase cell collisions creating larger particles while also keeping them constantly suspended (Shanks and Edmondson, 1989). We quantified incorporation of this particulate material by individual bacterial taxa using Chip-SIP, a method that uses stable isotope labeling, hybridization of RNA to phylogenetic microarrays, and isotopic imaging of the arrays using high-resolution secondary ion mass spectrometry (SIMS) with a Cameca NanoSIMS 50 (Mayali et al., 2012).

## MATERIALS AND METHODS

### Production of $^{15}\text{N}$ and $^{13}\text{C}$ Labeled Diatom-Derived Particles

We used  $^{15}\text{N}$  and  $^{13}\text{C}$  labeled phytodetrital particles from the diatom *Thalassiosira pseudonana* CCMP 1335 as a representative of phytoplankton-derived organic matter that is likely to reflect the composition of natural particles in the ocean, and dead algal detritus in algal biofuel production ponds. Cultures of

the *T. pseudonana* CCMP 1335 were grown in *F/2* medium (Guillard, 1975) with  $^{15}\text{NO}_3^-$  under continuous light at 20°C. To maximize the incorporation of labeled carbon, bottles containing the medium were tightly shut immediately after autoclaving to prevent equilibration with atmospheric air, and once cooled were bubbled with  $\text{N}_2$  gas for 10 min to remove  $^{12}\text{CO}_2$ . 99% atm%  $^{13}\text{C}$  labeled sodium bicarbonate ( $\text{NaH}^{13}\text{CO}_3$ ) was added at a concentration of 2 mM. A 100  $\mu\text{L}$  inoculum of *T. pseudonana* already growing in  $^{13}\text{CO}_2$  and  $^{15}\text{NO}_3$  medium was added and the cultures were incubated with the bottle cap shut. After early stationary phase of growth was achieved (approximately 2 weeks since the beginning of the experiment), cultures were centrifuged at 1,200 g, the liquid removed, and the pellet washed twice in filtered seawater, and frozen at  $-80^\circ\text{C}$ . Pellets were thawed and refrozen four times and washed in filtered artificial seawater to remove DOM from lysed cells, and frozen again before the start of the incubation experiment.

## Experimental Setup, DOC Analyses, and Bacterial Counts

Surface seawater from the Coastal Pacific was collected at the San Pedro Ocean Time Series (SPOT) Microbial Observatory site ( $33^\circ 33'\text{N}$ ,  $118^\circ 24'\text{W}$ ) on May 22nd of 2013 and taken to the laboratory within 4 h in a temperature-controlled container. The seawater was subsequently gently filtered to remove grazers and 5  $\mu\text{m}$  particles (5  $\mu\text{m}$  pore-size polycarbonate filters, Millipore Corp., Billerica, MA, United States), and then distributed into 10 polycarbonate 2-L cylindrical bottles (Nalgene). SIP-addition treatments were enriched with 0.19 g/L dry weight diatom-derived  $^{13}\text{C}$  and  $^{15}\text{N}$  labeled particles and incubated in the light (at 150  $\mu\text{mol m}^{-2} \text{s}^{-1}$ ) or in the dark in triplicate at 18°C in a rolling bottle setup at 0.5 rpm (CellRoll, Inc.). Duplicate control treatments with no added particles were incubated in the same temperature-controlled chamber in the light or dark in static bottles. Samples for cell counts, dissolved organic carbon (DOC), DNA and RNA were collected after 72 h in addition to  $T_0$ . While previous studies have shown that incubations of 12 h are sufficiently long to detect isotope incorporation with Chip-SIP (Mayali et al., 2012), we decided on 72 h incubations to allow the transfer of particulate C and N to the dissolved phase to occur. All material used was previously acid washed with 1% HCl and rinsed in double distilled water.

Samples for DOC were collected by filtering 100 ml of sample through 0.2  $\mu\text{m}$  pore-size polycarbonate filters (47 mm, Millipore Corp., Billerica, MA, United States). All material in contact for those samples was pre-rinsed with 1 M HCl. DOC samples were sent to the Nutrient Analysis Lab at University of Maryland for analysis. Samples for bacterial counts were preserved in 10% formalin and kept at 4°C until processing. Two milliliters of the formalin-fixed samples were stained using acridine orange (Hobbie et al., 1977), filtered onto 0.2  $\mu\text{m}$  pore-size black polycarbonate Track-Etched (PCTE) filters (25 mm, Fisher Scientific) and counted with epifluorescence microscopy. Samples for DNA and RNA were collected on 5  $\mu\text{m}$  pore size polycarbonate filters (47 mm, Millipore Corp., Billerica, MA, United States), representing large particles, henceforth referred to

as “particulate,” and the filtrate sequentially collected on 0.2  $\mu\text{m}$  pore size filters (47 mm diameter Durapore® Membrane Filters, Millipore Corp., Billerica, MA, United States), representing free-living microbes and those attached to small particles, henceforth referred to as “free-living.”

## Nucleic Acid Extraction, and Sequencing

RNA and DNA from particles ( $>5 \mu\text{m}$ ) and free-living bacteria (0.2–5  $\mu\text{m}$ ) from all replicates was extracted with the Qiagen AllPrep kit according to manufacturer's instructions for bacterial nucleic acid, using 10 mg/mL lysozyme in the lysis step and including vortexing for 10 min. Microbial diversity in the different treatments and size fractions was assessed by amplifying the V4 and V5 region of the 16S rRNA gene from the DNA extracts using primers 515F and 926R, and paired end 2 × 300 sequencing on MiSeq (Illumina; Parada et al., 2016). In addition to bacterial and archaeal 16S rRNA gene sequences, these primers also amplify chloroplastic 16S rRNA gene sequences and eukaryotic 18S rRNA gene sequences (Needham and Fuhrman, 2016; Parada et al., 2016), allowing determination of the relative ratios of rRNA genes within the domains Bacteria and Archaea to those of Eukarya. Demultiplexed sequences were quality filtered with Trimmomatic (Bolger et al., 2014), trimming reads with the following settings: SLIDINGWINDOW:5:30, MINLEN:250. Paired end reads were then merged with `usearch fastq_mergepairs` with the following settings: `-fastq_truncqual 5 -fastq_maxdiffs 0 -fastq_minmergelen 200 -fastq_minovlen 50` (Edgar, 2010). Only 16S rRNA gene sequences are merged at this step, as the 18S rRNA amplicons in this region are about 200 bp longer and as such do not overlap (see below). For merged sequences, primer sequences were removed with `cutadapt` (Martin, 2011). Chimeric sequences were identified in QIIME (Caporaso et al., 2010) with `identify_chimeric_seqs.py` using a *de novo* and referenced based approach using the `usearch61` method and the SILVA GOLD database (Quast et al., 2013). Operational taxonomical units (OTU) were determined using the `uclust` in QIIME with 99% similarity cutoffs. The most abundant sequence within each OTU was selected as a representative sequence. Each representative sequence was assigned classification with `QIIME assign_taxonomy.py` against the SILVA 111 database via the `uclust` algorithm. OTUs classified as chloroplastic at this step were then further classified with `Phyloref`.

After processing of the overlapped reads for 16S rRNA analyses, in order to assess the number of eukaryotic reads in our dataset, we searched all individual paired reads against separate 18S and 16S rRNA gene database from SILVA and selected the paired reads with a higher percent similarity to the 18S dataset compared to the 16S via `bbsplit.sh`<sup>1</sup>. Then the sequences were concatenated with an N separating the two reads and OTUs were generated as previously described (Needham and Fuhrman, 2016). The OTUs were classified in QIIME via the RDP classifier (Wang et al., 2007) against the PR2 database (Guillou et al., 2013).

For identification of bacterial and archaeal 16S rRNA gene sequence OTUs that were significantly more or less abundant in the different treatments and controls, we used the software

<sup>1</sup><https://github.com/jcmcnch/eASV-pipeline-for-515Y-926R>

packages phyloseq (McMurdie and Holmes, 2013) and DESeq2 (Love et al., 2014). Biom tables of read counts produced from the QIIME pipeline were imported into R via *import\_biom* of the phyloseq package. For samples where technical replicates were available ( $n = 2$ ), the reads from the replicates were summed. Then, the phyloseq object was converted to *deseq2* objects via *phyloseq\_to\_deseq2* for each statistical comparison of interest (light vs. dark, large vs. small, and control vs. experimental treatment). For determination of differential abundance between the experimental treatments (i.e., light vs. dark, and large vs. small size fraction), all of the different treatments of the other factor were used (that is, for example, data from both size fractions were used to determine significant shifts in light vs. dark treatments). Significant differences were determined with the *DESeq* command using a “Wald” test and a “parametric” fitType (i.e., the default settings). Results were converted to a results table with the *DESeq results* command, retaining all results for further exploration (i.e., *cooksCutoff = F*). Significant shifts were identified as those with a Benjamini–Hochberg adjusted  $p$ -value  $< 0.05$ . Heatmaps were generated with the program “heatmap3” in R. Phylogenetic trees were generated by alignment with MUSCLE (-maxiters 100; Edgar, 2004) and maximum likelihood tree generation with phym1 (Guindon et al., 2010). Those included amplicon representative sequences from the experimental taxa, together with relevant environmental sequences of previously reported phytoplankton bloom responders at SPOT (Needham and Fuhrman, 2016; Needham et al., 2018) and whole genome sequenced bacteria.

## Probe Design

We aimed to target organisms commonly found at SPOT as well as those that commonly become enriched on diatom-derived particles. For the former, sequences collected at SPOT were obtained from published literature (Brown et al., 2005; Needham et al., 2013). For the latter, we used probes from a previous Chip-SIP study that targeted dead *T. pseudonana* particle attached bacteria (Mayali et al., 2016). For probes targeting both diatom detritus and SPOT sequences, trimmed sequences were manually checked for quality and submitted to DECIPHER's Find Chimeras web tool (Wright et al., 2012), aligned with the online SINA aligner (Pruesse et al., 2007) and imported into SILVA database SSU\_NR ver. 103 in the ARB software (Ludwig et al., 2004), which included 263,000 small subunit ribosomal RNA sequences. Sequences were added to the global phylogeny and 148 unique operational taxonomic units (OTUs) were identified. For each OTU, a set of 25 probes targeting the OTU and closely related sequences were designed (**Supplementary Table S1**) using the probe design function in ARB. In most cases, probes were allowed to perfectly match with less than 5 sequences outside the targeted group (preferably none, but this was not always possible). Also, in most cases we required that two base-pair changes on the probe sequence (i.e., mismatches) did not match more than 100 sequences outside the targeted group. Our approach was to have multiple probes for each taxon, including probes that target the same region but are offset by a few bases in either direction. This leads to a range of probe melting temperatures for each taxon, and decreases the

likelihood that a single probe exhibits non-specific signal. The isotope enrichment of taxa was subsequently compared among one another in relation to the probe hybridization strength, as further explained below.

## Chip-SIP Analyses

RNA samples were split: one fraction saved for fluorescent labeling, the other was unlabeled for NanoSIMS analysis. Fluorescent Alexafluor 532 labeling was carried out with the Ulysis kit (Invitrogen) for 10 min at 90°C (2  $\mu$ L RNA, 10  $\mu$ L labeling buffer, 2  $\mu$ L Alexafluor reagent), followed by fragmentation. All RNA (fluorescently labeled or not) was fragmented using 1X fragmentation buffer (Affymetrix) for 10 min at 90°C before hybridization and concentrated by isopropanol precipitation to a final concentration of 500 ng  $\mu$ L<sup>-1</sup>. Glass slides coated with indium-tin oxide (ITO; Sigma) were coated with silane Super Epoxy 2 (Arrayit Corporation) to provide a starting matrix for DNA synthesis. Custom-designed microarrays (spot size = 17  $\mu$ m) were synthesized using a photolabile deprotection strategy (Singh-Gasson et al., 1999) by Roche Nimblegen (Roche Nimblegen, Madison, WI, United States). Reagents for synthesis (Roche Nimblegen) were delivered through the Expedite (PerSeptive Biosystems) system. For array hybridization, RNA samples (1  $\mu$ g) in 1X Hybridization buffer (Roche Nimblegen) were placed in Nimblegen X12 mixer slides and incubated inside a Maui hybridization system (BioMicro® Systems) for 18 h at 42°C and subsequently washed according to manufacturer's instructions (Roche Nimblegen). Arrays with fluorescently labeled RNA were imaged with a Genepix 4000B fluorescence scanner at pmt = 650 units. Secondary ion mass spectrometry analysis of microarrays hybridized with rRNA from the <sup>13</sup>C- and <sup>15</sup>N-labeled particle incubations was performed at LLNL with a Cameca NanoSIMS 50 (Cameca, Gennevilliers, France). A Cs+ primary ion beam was used to enhance the generation of negative secondary ions. Carbon isotopic ratios were determined on electron multipliers in pulse counting mode, measuring <sup>12</sup>C<sup>14</sup>N<sup>-</sup> and <sup>12</sup>C<sup>15</sup>N<sup>-</sup> simultaneously, and then <sup>12</sup>C<sup>14</sup>N<sup>-</sup> and <sup>13</sup>C<sup>14</sup>N<sup>-</sup> simultaneously. More details of the instrument parameters are provided elsewhere (Mayali et al., 2012). Ion images were stitched together, processed to generate isotopic ratios, and regions of interests (ROIs) of the individual probe spots extracted with the L'IMAGE software (L. Nittler, Carnegie Institution of Washington). Data were corrected for the background isotope ratios measured on probe spots hybridized with control oligonucleotides. For fluorescence, triplicate samples were combined and hybridized on the same microarray (4 total samples: FL dark, FL light, AT dark, and AT light). For NanoSIMS, all replicates were analyzed separately (12 total samples). We determined what OTUs in the different treatments were statistically isotopically enriched as described below. For each OTU and for each replicate of all treatments, <sup>15</sup>N enrichment (in permil) of individual probe spots was plotted versus fluorescence and a linear regression slope, which we refer to as the hybridization-corrected enrichment (HCE), was calculated. We carried out this calculation with the <sup>15</sup>N data as the <sup>13</sup>C exhibits higher background and thus lower signal to noise. OTUs were considered significantly isotopically enriched

if the slope minus two calculated standard errors (SE) was greater than zero and if the slope was significant based on a *t*-score statistic ( $t = \text{slope}/\text{SE}$ ) with a *p*-value of less than 0.05 adjusted with the Benjamini–Hochberg false discovery rate procedure. We considered an OTU enriched in a particular treatment if two out of three replicates were statistically significantly enriched.

The second type of analysis tested differential isotope labeling of the same probes with an analysis of covariance (ANCOVA) using the software JMP v.8.0 (Statistical Discovery™). This method applies a standard least squares approach to determine if the treatment significantly affected the slope of enrichment over fluorescence. We tested the effect of light, both for free-living and attached fractions, as well as the effect of attachment, both for light and dark incubated samples, on the HCE slope. The treatment effect (either light vs. dark or particle vs. free-living) was used as an “independent effect” or “interaction effect” on the relationship between fluorescence and isotope enrichment. In these analyses, the model tested the contributions of three components on the isotope enrichment: (1) the experimental treatment (e.g., light vs. dark or attached vs. free-living), (2) the fluorescence, and (3) the interaction of treatment and fluorescence, so called the crossed effect. We used this latter component (the interaction effect) as an indication of the treatment having a significant effect on the isotope incorporation.

## RESULTS

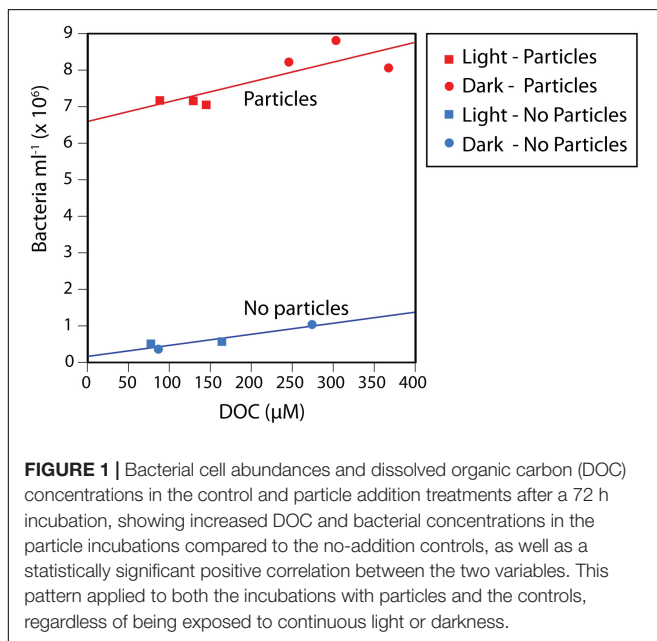
### Microbial Community Response to Particles

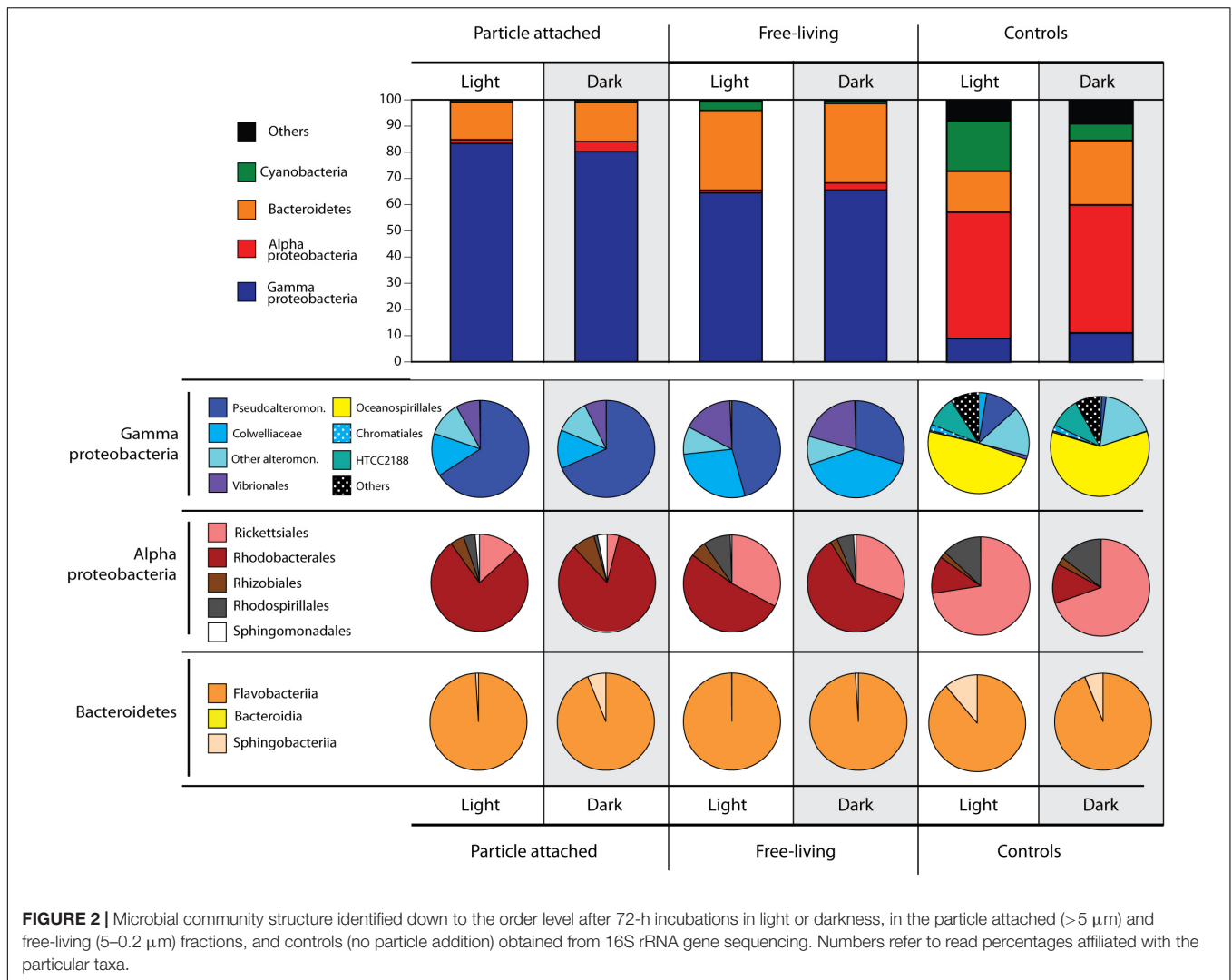
Following the 72-h incubation of Pacific Ocean microbial cells in the presence of phytodetrital particles, both cell and DOC concentrations increased compared to the control (no particle) incubations (Figure 1). Cell and DOC concentrations were

positively correlated with one another for both control ( $r = 0.95$ ,  $p = 0.05$ ) and particle ( $r = 0.83$ ,  $p = 0.04$ ) incubations, suggesting that higher DOC concentrations supported increased microbial growth and vice versa. Furthermore, the dark particle incubations exhibited significantly higher cell abundances (15% increase,  $p = 0.006$ ) and DOC concentrations (65% increase,  $p = 0.01$ ) compared to the light incubations. The particles remained visibly larger and greener after incubation in the dark (Supplementary Figure S1), suggesting that light-enhanced chlorophyll degradation occurred in the light treatment, as previously observed (Rontani, 2001; Mayer et al., 2009).

A total of 348,385 high-quality, merged 16S rRNA reads were obtained from 15 samples. After removal of chimeras (1.2% of sequences) and singletons, we obtained 1,262 OTUs clustered at 99%, including 592 that were detected in the particle-addition treatments. The majority of sequences were classified into the domains Bacteria or Archaea (99.23–99.80%), while 0.05–0.99% were eukaryotic or belonged to chloroplasts (Supplementary Table S2). Microbial communities in all incubations were dominated by Gammaproteobacteria (Figure 2), and this was more pronounced in the particle-attached fraction (>80% OTUs) compared to the free-living (~65%). The clearest patterns of differential abundance were OTUs numerically enriched in the particle treatments compared to the controls (which were numerically dominated by SAR11 OTUs; Figure 2 and Supplementary Figure S2). The particle enrichment treatments experienced a clear shift in community composition (Figures 2, 3) with increased numbers of OTUs belonging to Flavobacteriales, Rhodobacterales, Alteromonadales, and Vibrionales (Figure 2 and Supplementary Figure S2). In general, these taxa are known copiotrophs (Buchan et al., 2014) commonly found to be associated with naturally occurring particles in marine samples, thus we focus the rest of our analyses on the specific taxa with distinct distribution patterns within the particle addition treatments.

Several differences between the free-living vs. particle-attached fractions were identified in the particle addition treatments (Figure 2). Within the Gammaproteobacteria, Pseudoalteromonadaceae OTUs were in significantly higher relative abundances attached to particles compared to free-living, and also higher in the light compared to the dark. Conversely, Colwelliaceae and Vibrionales abundances increased in the free-living fractions compared to the attached fraction. Bacteroidetes were the second most abundant group detected in our samples. In contrast to many of the Gammaproteobacteria, the relative abundance of Bacteroidetes was twice as high in the free-living fractions (~30%) compared to the particle attached fractions (~15%). Within Bacteroidetes, >95% of the OTUs belonged to Flavobacteriia, with 5% of the reads belonging to Sphingobacteriia exclusively found in the dark particle-attached treatment (Figure 2). Alphaproteobacteria and Cyanobacteria were the taxa with the overall lowest abundances in the particle addition treatments (Figure 2). Alphaproteobacteria OTU abundances were higher in the dark treatments, Rhodobacterales being the most abundant, especially in the particle-attached treatments (>75% of all





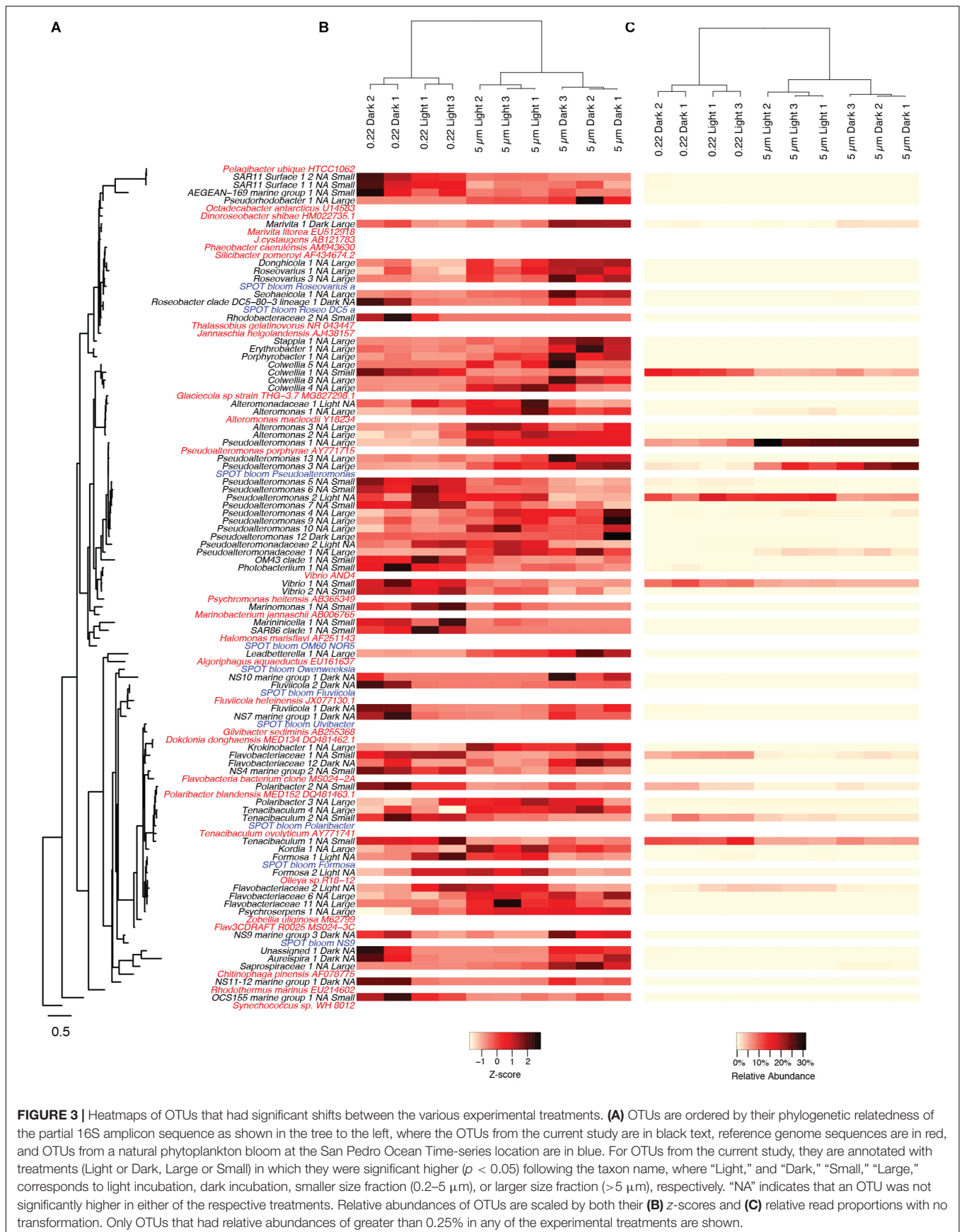
Alphaproteobacteria) compared to the free-living (50–60%). Also within Alphaproteobacteria, the Rickettsiales were most abundant in the free-living fractions of both light and dark incubations. Cyanobacteria were detected only in the light free-living samples.

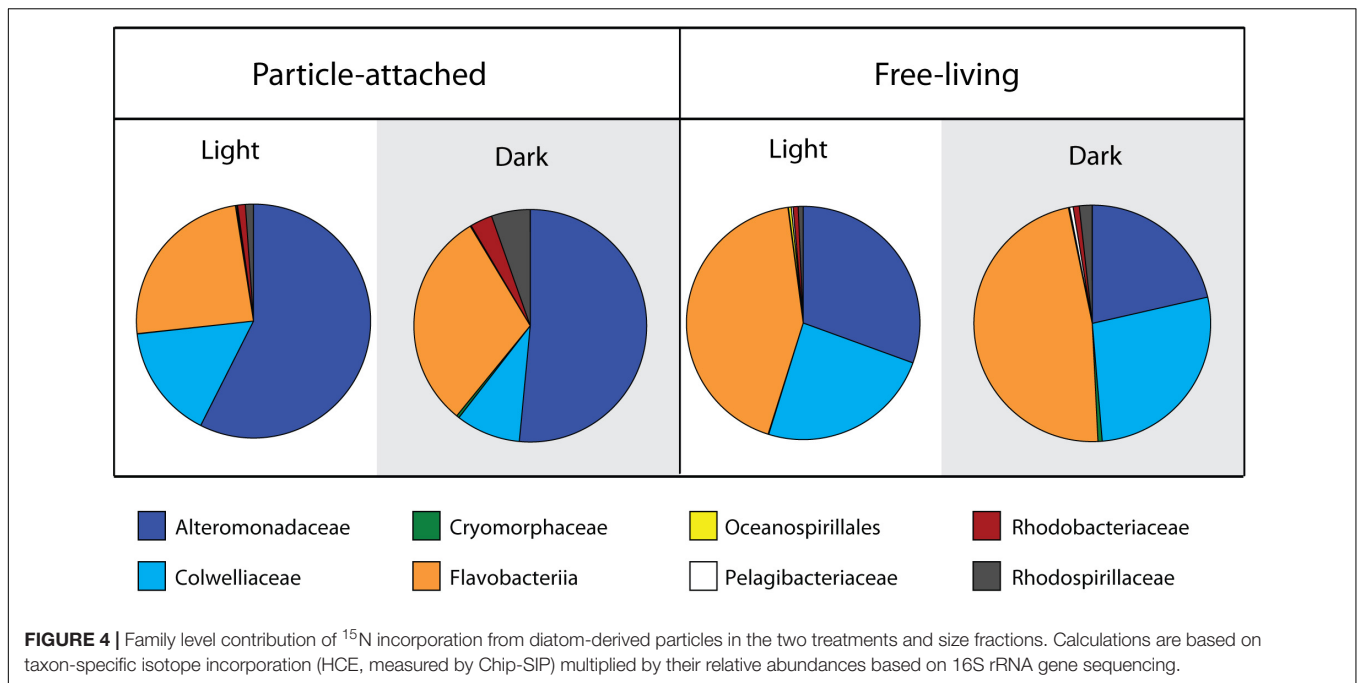
The patterns described above at higher taxonomic levels were mainly driven by the appearance of individual OTUs from those taxa. Many OTUs significantly responded to light regime, particle attachment, or both (adjusted  $p < 0.05$ , **Figure 3**). A total of 6 OTUs were numerically enriched in the light treatments, including 3 Flavobacteriales and 2 Alteromonadales. We also identified 12 OTUs numerically enriched in the dark treatments, including 6 Flavobacteriales and 2 Rhodobacterales. Within the particle incubations, 32 OTUs were numerically enriched in the large particle fractions (>5  $\mu\text{m}$ ), including 12 Gammaproteobacteria and 8 Flavobacteria. Twenty-one OTUs were numerically enriched in the smaller size fraction (5–0.22  $\mu\text{m}$ ), including 2 SAR11, 10 Gammaproteobacteria, and 5 Flavobacteria. Of the above mentioned OTUs, only two were significantly enriched in specific combinations of light regime

and particle attachment: one Rhodobacterales (*Marivita* sp.) and one Pseudoalteromonas OTU, both as particle attached in the dark (**Figure 3**).

### Incorporation of Isotope Labeled Particulate Organic Matter

Out of a total of 156 OTUs targeted by the microarrays, 53 OTUs were not isotopically enriched in any of the 12 samples, and another 7 were not enriched in at least two replicates of the same treatment (**Supplementary Figure S3**). This is a common phenomenon documented in previous Chip-SIP studies (Mayali et al., 2012) as well as density gradient SIP (Dumont and Murrell, 2005). These unenriched taxa represent organisms that were either (i) in extremely low abundance in the samples or not present at all, (ii) present in the sampled seawater but not growing in the bottled incubations, or (iii) growing but did not incorporate C and N derived from the particles. We focus our subsequent data analyses and discussions on taxa that significantly incorporated





labeled C and N from the particles. Most OTUs significantly enriched based on our criteria were, indeed, labeled in all treatments and size fractions (i.e., attached, free-living, light, and dark). This shows that within the 72-h incubation, particulate C and N was incorporated by both attached and free-living bacteria, and that this occurred both in the dark and in the light.

To obtain a taxonomic breakdown of particle-derived isotope incorporation from the different incubations and size fractions, we took the HCE values (corresponding to relative isotope incorporation) for each OTU for all replicates and averaged those values across the most abundant bacterial families. This calculation represents the relative isotope incorporation for each family, but does not take into account the abundances of those families in the samples. In order to estimate their total contribution to particulate N incorporation, we multiplied the relative isotope incorporation for each family by the percentage of reads corresponding to that family found in each of the treatments and size fractions. These calculated values should approximate the amount of isotope assimilated by the respective families in the four sample types (**Figure 4**), if we assume that 16S rRNA gene read abundances correspond to relative abundances in the samples. The patterns of stable isotope incorporation in the different treatments were similar to those observed in the overall microbial community structure, retrieved by 16S iTAG sequencing. We found that the families Alteromonadaceae, Flavobacteriaceae, and Colwelliaceae dominated the isotope incorporation in the two experimental treatments with added particles. In the attached fractions, the Alteromonadaceae was particularly dominant, responsible for greater than 50% of the incorporation, both in the dark and light treatment. On the other hand, in the free-living fractions,

the Flavobacteriaceae dominated isotope incorporation (48% in the dark incubations and 43% in the light; **Figure 4**). As also observed by iTAG sequencing, the family Colwelliaceae incorporated the isotope mostly in the free-living fractions (24–27%) compared to the particle attached (9–16%). Other less abundant families contributed less than 1% of the isotope incorporation, with the exception of Rhodospirillaceae (5%) and Rhodobacteriaceae (3%) in the attached fraction of the dark treatment.

### Influence of Light on Isotope Incorporation

Using covariance analysis (ANCOVA, **Supplementary Figure S4**), we tested which OTUs exhibited significantly distinct isotope labeling patterns according to treatment (light vs. dark) and size fraction (free-living vs. attached; **Table 1**). These represent taxa with significant treatment and fluorescence crossed effects on isotope labeling, with adjusted  $p$ -values  $<0.05$ . We identified six particle-attached OTUs that incorporated significantly more isotope in the light compared to the dark. These OTUs represented some of the most abundant taxa found in the samples according to the 16S rRNA gene sequencing data, and included the genera *Pseudoalteromonas*, *Colwellia*, and members of the Flavobacteriaceae family. One of the Flavobacteriaceae OTU (*Owenweeksia*) was the only OTU that also exhibited increased incorporation in the light-incubated free-living samples compared to the dark-incubated samples. Seven other OTUs exhibited the opposite pattern when attached to particles, with significantly higher isotope incorporation in the dark. These included less abundant taxa, such as OTUs from the Oceanospirillales, Rhodospirillales, uncultured Flavobacteriaceae, uncultured

**TABLE 1** | Summary of covariance analysis (ANCOVA) results showing OTUs with statistically significant treatment differences for incorporation of <sup>15</sup>N from particles.

OTU	Taxonomy	GB accession	Particle attached		Free-living	Light	Dark
			Higher in light	Higher in dark	Higher in Light	Higher in free-living	Higher in free-living
Owenweeksia_B	Bacteria;Bacteroidetes;Flavobacteria_Flavobacteriales;Cryomorphaceae_Owenweeksia	KC287128	X		X		X
Colwellia_IA	Bacteria;Gammaproteobacteria;Alteromonadales_1;Colwelliaceae;Colwellia_1	KC287092	X			X	X
Pseudoalteromonas_A	Bacteria;Gammaproteobacteria;Alteromonadales_1;Pseudoalteromonas	KC287096	X				X
Maribacter	Bacteria;Bacteroidetes;Flavobacteria_Flavobacteriales;Flavobacteriaceae_1; Maribacter	KC287125	X				X
Colwellia_IB	Bacteria;Gammaproteobacteria;Alteromonadales_1;Colwelliaceae;Colwellia_1	KC287093	X				X
Flavobacterium_IB	Bacteria;Bacteroidetes;Flavobacteria_Flavobacteriales;Flavobacteriaceae_1;	KC287124	X				
890_1_C_2	Bacteria;BD1-5	KF227631		X		X	X
890_1_E_8	Bacteria;Gammaproteobacteria;Legionellales;Legionellaceae; uncultured	JF767288		X		X	
SPOTSMAY03_890m27	Bacteria;Gammaproteobacteria;Oceanospirillales;Oceanospirillaceae;Pseudospirillum	DQ009470		X			
SPOTSAPR01_5m177	Bacteria;Gammaproteobacteria;Oceanospirillales;OM182 clade	DQ009128		X			
890_2_B_8	Bacteria;Actinobacteria;Acidimicrobia;Acidimicrobiales;Sva0996 marine group	KF227626		X			
890_1_G_6	Bacteria;Bacteroidetes;Flavobacteria;Flavobacteriales;Flavobacteriaceae; uncultured	KY282445		X			
890_1_G_2	Bacteria;Alphaproteobacteria;Rhodospirillales;Rhodospirillaceae; uncultured	KF227741		X			
SPOTSMAY03_890m21	Bacteria;Gammaproteobacteria;Alteromonadales;Alteromonadaceae;SAR92 clade	DQ009469				X	X
SPOTSAUG01_5m75	Bacteria;Gammaproteobacteria;Thiotrichales;Piscirickettsiaceae; uncultured	DQ009136				X	X
Oceanobacter_A	Bacteria;Gammaproteobacteria;Oceanospirillales_Oceanospirillaceae_2;Oceanobacter	KC287100				X	X
Maritalea	Bacteria;Alphaproteobacteria;Rhizobiales_1; Hyp homicrobiaceae; Maritalea	KC287120				X	X
Glaciecola_I	Bacteria;Gammaproteobacteria;Alteromonadales_1;Alteromonadaceae_1;Glacie cola	KC287090				X	X
Clostridium	Bacteria;Firmicutes;Clostridia_1;Clostridiales;Ruminococcaceae; uncultured	KC287133				X	X
Alcanivora_AB	Bacteria;Gammaproteobacteria;Oceanospirillales_Alcanivoraceae_Alcanivora	KC287107				X	X
890_2_F_10	Bacteria;Proteobacteria;CF2	KF227740				X	X
SPOTSAPR01_5m148	Bacteria;Deferribacteres;Deferribacteres;Deferribacterales;SAR406 clade (Marine group A)	DQ009148				X	
SPOTSAPR01_5m105	Bacteria;Alphaproteobacteria;Rhodobacterales_Rhodobacteriaceae_1; uncultured	DQ009158				X	
890_4_D_5	Bacteria;Lentisphaerae;Lentisphaeria;Lentisphaerales;Lentisphaeraceae;Lentisphaera	AB703829				X	
890_4_B_7	Bacteria;Bacteroidetes;Flavobacteria;Flavobacteriales;NS9 marine group	KF227727				X	
Roseobacter_B	Bacteria;Alphaproteobacteria;Rhodobacterales_Rhodobacteriaceae_1; uncultured	KC287113					X
Oceaniserpentilla	Bacteria;Gammaproteobacteria;Oceanospirillales_Oceanospirillaceae_2;Oceaniserpentilla	KC287102					X
JTB148	Bacteria;Gammaproteobacteria;JTB148	KC287110					X
Hyphomonas	Bacteria;Alphaproteobacteria;Caulobacter_Hyphomonadaceae; Hyphomonas; Hyphomonas_1	KC287118					X
Colwellia_2	Bacteria;Gammaproteobacteria;Alteromonadales_1;Colwelliaceae;Colwellia_2	KC287094					X
890_2_G_S	Bacteria;Alphaproteobacteria;Rhodospirillales;Rhodospirillaceae;Defluviococcus	KF227655					X

Several examples are shown in more detail in **Supplementary Figure S4**.

Legionellaceae, and the Sva0996 marine group from the Actinobacteria. The remaining OTUs showing differential isotope incorporation were exclusively more enriched in the free-living compared to the particle attached phase (Table 1). Some of these taxa exhibited differential labeling patterns both in the light and in the dark, or in one but not the other treatment.

## DISCUSSION

Our experimental setup was designed to use a taxon-specific, isotope labeling method (Chip-SIP) to quantify C and N incorporation by bacteria colonizing phytodetrital particles in laboratory incubations. We used freeze-thawed diatoms as model phytodetrital particles, an approach carried out in a number of previous studies (Bidle and Azam, 1999; Ploug, 2001), as they mimic natural sources of particulate C and N, which are degraded by microbial communities as they sink in the ocean. These types of studies are also valuable to understand the fate of algal detritus in outdoor raceway ponds used for biofuel production (Milledge and Heaven, 2013). To our knowledge, this is the first such study to utilize stable isotope labeling of the particulate algal material to trace its fate through the community. We added the impact of light in our experimental design to further examine how photoheterotrophic processes affect C and N cycling as bacteria colonized the particles. Different OTUs responded to all possible combinations of particle attachment vs. free-living lifestyle under light or dark conditions, at the level of 16S rRNA gene relative abundances. We further observed that some of these taxa showed differential labeling patterns, some in the light and others in the dark, as well as differential labeling between free-living and attached. The most common pattern was higher isotope incorporation in the free-living phase compared to attached (Table 1). This finding was initially rather puzzling since the isotope labeling originated from the particles and we expected isotope incorporation to be greater when the bacteria were particle-attached. However, previous work has shown that particle-attached bacteria exhibit greater per-cell enzyme activities but slower growth compared to their free-living counterparts, in other words, a decoupling between enzyme hydrolysis and uptake (Unanue et al., 1998; Beier and Bertilsson, 2011). Furthermore, some of the taxa responsible for the first stages of particle degradation might have later been transferred to the small fraction after 72 h, as we discuss below.

### Bacterial Dynamics of Phytodetrital Particle Degradation

Bacterial growth dynamics that follow algal blooms involve sequential steps of particle breakdown that are performed by different members of the microbial community. Consistent with our findings of Alteromonadaceae playing a major role in particle degradation, Sarmiento and Gasol (2012) found that *Alteromonas* dominated the uptake of radiolabeled diatom particles during 24-h incubations. However, the first taxa to

colonize phytodetrital particles after 5 h were members of the Flavobacteria. Several other studies also identified Flavobacteria as the first and major taxa consuming algal bloom biomass (Kirchman, 2002; Gómez-Pereira et al., 2012; Williams et al., 2013). The length of our incubations (72 h) did not allow identifying the taxa that initially attached to the diatom particles. Although previous studies have shown that incubations of 12 h are sufficiently long to detect isotope incorporation with Chip-SIP (Mayali et al., 2012), we decided on extended incubations of 3 days to allow the transfer of particulate C and N to the dissolved phase to occur. Therefore, members of the Flavobacteria may have been, indeed, the first taxa to respond in our incubations. These initial steps potentially involved bacterial attachment to particles, complex organic matter degradation using exoenzymes (Kirchman, 2002; Teeling et al., 2012) and the release of smaller breakdown products. After this first response, Flavobacteria would have increased their relative abundances in the small fraction while the Alteromonadales dominated on particles, potentially taking advantage of less complex organic molecules produced by the Flavobacteria. We further hypothesize that this process may have been more efficient in the light due to proteorhodopsin photoheterotrophy. This would be consistent with the high relative abundance of flavobacterial rhodopsin genes and transcripts found in particle-associated natural samples from surface waters (Maresca et al., 2018). Additionally, Flavobacteria TonB transporters rely on proton gradients and have been shown to be highly expressed during the peak of algal blooms (Teeling et al., 2012), suggesting a role of PR electrochemical gradients in these transport processes (Gómez-Consarnau et al., 2016). It therefore seems plausible that, in the marine environment, the first stages of diatom biomass degradation would generally be carried out mostly by photoheterotrophic Flavobacteria still within the photic zone, and that the subsequent stages of organic matter degradation would take place regardless of light as particles sink below the photic zone. Overall, there are numerous cooperative processes among members of the microbial community to accomplish the ultimate degradation of phytodetrital material, as suggested for other microbial processes in the ocean (Morris et al., 2012). Future research tracking down the transfer of biomass at different stages of an algal bloom will be necessary to better identify the role of photoheterotrophy in these first steps of algal biomass degradation.

### Light-Induced Microbial Community Response to Organic Particles

One of the goals of this study was to identify the microbial taxa that occupy different niches as consumers of marine organic matter in the photic zone. These include (i) particle-attached phototrophs, which would take advantage of light through photoheterotrophy to enhance the transport and uptake of complex particulate organic matter, (ii) particle-attached chemoheterotrophs, which include decomposers of labile complex organic matter in particles without using light, (iii) free-living phototrophs, which are bacterial groups potentially

specialized in the light-mediated utilization of smaller organic molecules that remain in seawater after being released from different sources (e.g., particle dissolution, viral lysis) and (iv) free-living chemoheterotrophs, which solely rely on dissolved organic matter utilization. Using our experimental incubation approach and examining the relative abundance of 16S rRNA genes and isotope incorporation differences between treatments, we were able to identify several patterns of niche preference at various taxonomic levels, including some that were only detected at the OTU level.

### Particle-Attached Chemoheterotrophs vs. Photoheterotrophs

Taxa in the family Alteromonadaceae clearly dominated the phytodetrital particle enrichments with some OTUs with higher relative abundances in the attached microbial fraction and others in the free-living. Light regime, however, did not have an effect on their overall abundances (except for two OTUs with greater abundances in the light treatment). Isotope incorporation for several OTUs from this family, however, was greater in the light compared to the dark. Alteromonadaceae are known for their opportunistic lifestyles and rapid growth responses on pulses of organic matter (Allers et al., 2007). There are virtually no phototrophs known in this family (Pinhassi et al., 2016), which would explain the general lack of growth response to light regime in our incubation experiments. Increased isotope incorporation in the light, however, could have been a result of (i) photolysis of the phytodetrital particles (Mayer et al., 2009) or (ii) other microbial taxa using photoheterotrophy to start degrading high molecular weight compounds. These two processes could potentially increase the availability of newly produced low molecular DOM for the Alteromonadaceae. Thus, our data are consistent with the idea that a light-mediated process can lead to an increased C and N transfer to non-phototrophic bacteria.

A number of other OTUs, including members of the orders Oceanospirillales, Rhodospirillales, and other Flavobacteriales, on the other hand, incorporated relatively more isotope and some of them were more abundant in the particle-attached dark treatment compared to the light. These taxa may be inhibited by light or the combination of light and organic matter availability, which can cause the formation of reactive oxygen species. While light wavelengths within the visible spectrum range have been shown to stimulate the overall bacterial activity at the community level, certain bacterial groups may experience light inhibition (reviewed by Ruiz-González et al., 2013). Interestingly, the majority of the taxa with higher isotope incorporation in the dark correspond to sequences originally sampled from the deepest SPOT station (890 m depth; **Table 1**), consistent with the notion that these taxa are better adapted to dark conditions.

One surprising result from the isotope incorporation and the relative abundance data was the lack of an effect of light on the family Rhodobacteriaceae. Many of these taxa are aerobic anoxygenic phototrophs, using bacteriochlorophyll to harvest light energy (Koblížek, 2015). While several studies show that light seldom stimulates their growth (e.g., Ferrera et al., 2011),

it can increase their substrate uptake rates (Ferrera et al., 2017). Rhodobacteriaceae are also known to increase in abundance during phytoplankton blooms, presumably consuming freshly synthesized organic matter and often associated with particles (Buchan et al., 2014; Teeling et al., 2016). It is possible that due to our experimental setup consisting of 24-h continuous light incubations, photoheterotrophic metabolism by AAP bacteria may have been inhibited in the light, as bacteriochlorophyll is synthesized during the dark cycle (Wagner-Döbler and Biebl, 2006).

### Free-Living Chemoheterotrophs vs. Photoheterotrophs

A number of studies have now shown that free-living strict chemoheterotrophy is not the most successful metabolism in surface waters, as the majority of bacteria in these environments are known free-living photoheterotrophs containing genes for proteorhodopsin phototrophy (80–100% of picoplankton genomes) or aerobic anoxygenic photosynthesis (5–30% of genomes; Brindefalk et al., 2016; Dubinsky et al., 2017; Sieradzki et al., 2018). In this study, we identified several free-living OTUs that became numerically enriched in the light compared to the dark, and one that exhibited increased relative isotope incorporation in the light versus the dark. These included several Flavobacteria OTUs, a family with numerous representatives containing PR genes (e.g., Gómez-Consarnau et al., 2007; Gonzalez et al., 2008; Inoue et al., 2013; Yoshizawa et al., 2014). However, some other Flavobacteria OTUs were enriched in the dark treatments instead, suggesting a chemoheterotrophic lifestyle by those organisms. Indeed, not all marine Flavobacteria strains in culture contain PR genes in their genomes (Fernández-Gómez et al., 2013), and even the ones that do seem to only respond to light when organic matter is scarce and additional scavenging capacities are needed (Gómez-Consarnau et al., 2007, 2016). A key factor in this light-induced response is that the threshold at which a population experiences substrate limitation – by type of molecule and concentration – can be different from strain to strain (Hagström et al., 2017). Still, as discussed above, photoheterotrophic members of Flavobacteria may have been important in the first particle degradation steps of our light incubations. Our present experimental data cannot confirm this and future research will be needed to better understand their role on particle degradation. Nevertheless, our observations reflect a high functional complexity and regulation in members of Flavobacteria (as determined by 16S rRNA gene; Teeling et al., 2012). From an ecological perspective, these slight functional differences are likely vital to maintain separate niches in the microbial community, ultimately giving each OTU the potential to thrive in changing environmental conditions such as that experienced through an algal bloom rise and decay.

### Impact of Light on Organic Matter Utilization

Free-living bacterial cell and DOC concentrations were significantly lower in the light compared to the dark after

incubation with phytodetrital particles. This suggests that either light inhibited bacterial degradation of the particles, which would result in lower bacterial growth and less dissolution of POC into DOC, or light induced more efficient particle degradation due to photoheterotrophic metabolism. In the latter case, labile carbon in the light was either being (i) incorporated into larger cells or (ii) respired at a higher rate. Since we did not observe any obvious increases in cell size in the light, it seems more plausible that bacteria had, indeed, access to more C in the light and that more of this C was subsequently being respired. Experiments with proteorhodopsin-containing Flavobacteria strains have previously shown that light can enhance the uptake of certain organic molecules (i.e., vitamins, Gómez-Consarnau et al., 2016), which are required for growth, and therefore respiration. Under this scenario, a larger fraction of the organic matter pool would be accessible in the light due to light-enhanced DOM uptake and utilization. However, if we consider photoheterotrophy to be a dominant trait in this microbial community—as a whole—with the potential to increase bacterial fitness, it is puzzling that bacterial abundances were lower in the light incubations. Future research with a higher temporal resolution and more extensive C and N partitioning budgets will be needed to answer this question, and will require quantifying the stable isotopic signal in the particulate, dissolved and gas (i.e., CO<sub>2</sub>) fractions during light/dark incubations.

## REFERENCES

- Alderkamp, A.-C., Van Rijssel, M., and Bolhuis, H. (2007). Characterization of marine bacteria and the activity of their enzyme systems involved in degradation of the algal storage glucan laminarin. *FEMS Microbiol. Ecol.* 59, 108–117. doi: 10.1111/j.1574-6941.2006.00219.x
- Allers, E., Gómez-Consarnau, L., Pinhassi, J. H. J., Gasol, J. M., Šimek, K., and Pernthaler, J. (2007). Response of *Alteromonadaceae* and *Rhodobacteriaceae* to glucose and phosphorus manipulation in marine mesocosms. *Environ. Microbiol.* 9, 2417–2429. doi: 10.1111/j.1462-2920.2007.01360.x
- Azam, F., and Long, R. A. (2001). Oceanography - sea snow microcosms. *Nature* 414, 495–497. doi: 10.1038/35107174
- Beier, S., and Bertilsson, S. (2011). Uncoupling of chitinase activity and uptake of hydrolysis products in freshwater bacterioplankton. *Limnol. Oceanogr.* 56, 1179–1188. doi: 10.4319/lo.2011.56.4.1179
- Béjà, O., Aravind, L., Koonin, E. V., Suzuki, M. T., Hadd, A., Nguyen, L. P., et al. (2000). Bacterial rhodopsin: evidence for a new type of phototrophy in the sea. *Science* 289, 1902–1906. doi: 10.1126/science.289.5486.1902
- Bidle, K. D., and Azam, F. (1999). Accelerated dissolution of diatom silica by marine bacterial assemblages. *Nature* 397, 508–512. doi: 10.1038/17351
- Bolger, A. M., Lohse, M., and Usadel, B. (2014). Trimmomatic: a flexible trimmer for Illumina sequence data. *Bioinformatics* 30, 2114–2120. doi: 10.1093/bioinformatics/btu170
- Brindfolk, B., Ekman, M., Ininbergs, K., Dupont, C. L., Yooseph, S., Pinhassi, J. H. J., et al. (2016). Distribution and expression of microbial rhodopsins in the Baltic Sea and adjacent waters. *Environ. Microbiol.* 18, 4442–4455. doi: 10.1111/1462-2920.13407
- Brown, M. V., Schwalbach, M. S., Hewson, I., and Fuhrman, J. A. (2005). Coupling 16S-ITS rDNA clone libraries and automated ribosomal intergenic spacer analysis to show marine microbial diversity: development and application to a time series. *Environ. Microbiol.* 7, 1466–1479. doi: 10.1111/j.1462-2920.2005.00835.x

## AUTHOR CONTRIBUTIONS

LG-C and XM designed the study, did the incubation experiments, and processed the samples. DN did the iTAG sequence analysis. LG-C, DN, PW, JF, and XM analyzed data and contributed to the writing of the manuscript.

## FUNDING

Work performed by XM and PW was funded by the United States Department of Energy's Office of Biological and Environmental Research Biofuels Science Focus Area Grant SCW1039, and work at LLNL was performed under the auspices of the United States Department of Energy at the Lawrence Livermore National Laboratory under Contract DE-AC52-07NA27344. LG-C was funded by the Marie Curie Actions-International Outgoing Fellowships (project 253970) and the United States National Science Foundation grant OCE1335269.

## SUPPLEMENTARY MATERIAL

The Supplementary Material for this article can be found online at: <https://www.frontiersin.org/articles/10.3389/fmicb.2019.01204/full#supplementary-material>

- Buchan, A., LeCleir, G. R., Gulvik, C. A., and Gonzalez, J. M. (2014). Master recyclers: features and functions of bacteria associated with phytoplankton blooms. *Nat. Rev. Micro.* 12, 686–698. doi: 10.1038/nrmicro3326
- Caporaso, J. G., Kuczynski, J., Stombaugh, J., Bittinger, K., Bushman, F. D., Costello, E. K., et al. (2010). QIIME allows analysis of high-throughput community sequencing data. *Nat. Methods* 7, 335–336. doi: 10.1038/nmeth.f.303
- Church, M. J., Ducklow, H. W., and Karl, D. M. (2004). Light dependence of [3H]Leucine incorporation in the oligotrophic North Pacific Ocean. *Appl. Environ. Microbiol.* 70, 4079–4087. doi: 10.1128/AEM.70.7.4079-4087.2004
- Dubinsky, V., Haber, M., Burgsdorf, I., Saurav, K., Lehahn, Y., Malik, A., et al. (2017). Metagenomic analysis reveals unusually high incidence of proteorhodopsin genes in the ultraoligotrophic Eastern Mediterranean Sea. *Environ. Microbiol.* 19, 1077–1090. doi: 10.1111/1462-2920.13624
- Dumont, M. G., and Murrell, J. C. (2005). Stable isotope probing — linking microbial identity to function. *Nat. Rev. Microbiol.* 3, 499–504. doi: 10.1038/nrmicro1162
- Edgar, R. C. (2004). MUSCLE: multiple sequence alignment with high accuracy and high throughput. *Nucleic Acids Res.* 32, 1792–1797. doi: 10.1093/nar/gkh340
- Edgar, R. C. (2010). Search and clustering orders of magnitude faster than BLAST. *Bioinformatics* 26, 2460–2461. doi: 10.1093/bioinformatics/btq461
- Evans, C., Gómez-Pereira, P. R., Martin, A. P., Scanlan, D. J., and Zubkov, M. V. (2015). Photoheterotrophy of bacterioplankton is ubiquitous in the surface oligotrophic ocean. *Prog. Oceanogr.* 135, 139–145. doi: 10.1016/j.pocean.2015.04.014
- Fernández-Gómez, B., Richter, M., Schüler, M., Pinhassi, J. H. J., Acinas, S. G., Gonzalez, J. M., et al. (2013). Ecology of marine *Bacteroidetes*: a comparative genomics approach. *ISME J.* 7, 1026–1037. doi: 10.1038/ismej.2012.169
- Ferrera, I., Gasol, J. M., Sebastian, M., Hojerova, E., and Koblizek, M. (2011). Comparison of growth rates of aerobic anoxygenic phototrophic bacteria and other bacterioplankton groups in coastal mediterranean waters. *Appl. Environ. Microbiol.* 77, 7451–7458. doi: 10.1128/AEM.00208-11
- Ferrera, I., Sánchez, O., Kolářová, E., Koblizek, M., and Gasol, J. M. (2017). Light enhances the growth rates of natural populations of aerobic anoxygenic phototrophic bacteria. *ISME J.* 11, 2391–2393. doi: 10.1038/ismej.2017.79

- Geng, H., Sale, K. L., Tran-Gyamfi, M. B., Lane, T. W., and Yu, E. T. (2016). Longitudinal analysis of microbiota in microalga nannochloropsis salina cultures. *Microb. Ecol.* 72, 14–24. doi: 10.1007/s00248-016-0746-4
- Gifford, S. M., Sharma, S., Booth, M., and Moran, M. A. (2013). Expression patterns reveal niche diversification in a marine microbial assemblage. *ISME J.* 7, 281–298. doi: 10.1038/ismej.2012.96
- Giovannoni, S. J., Bibbs, L., Cho, J.-C., Stapels, M. D., Desiderio, R. A., Vergin, K. L., et al. (2005). Proteorhodopsin in the ubiquitous marine bacterium SAR11. *Nature* 438, 82–85. doi: 10.1038/nature04032
- Gómez-Consarnau, L., Gonzalez, J. M., Coll-Llado, M., Gourdon, P., Pascher, T., Neutze, R., et al. (2007). Light stimulates growth of proteorhodopsin-containing marine *Flavobacteria*. *Nature* 445, 210–213. doi: 10.1038/nature05381
- Gómez-Consarnau, L., Gonzalez, J. M., Riedel, T., Jaenicke, S., Wagner-Döbler, I., Sañudo-Wilhelmy, S. A., et al. (2016). Proteorhodopsin light-enhanced growth linked to vitamin-B1 acquisition in marine *Flavobacteria*. *ISME J.* 10, 1102–1112. doi: 10.1038/ismej.2015.196
- Gómez-Pereira, P. R., Hartmann, M., Grob, C., Tarran, G. A., Martin, A. P., Fuchs, B. M., et al. (2013). Comparable light stimulation of organic nutrient uptake by SAR11 and *Prochlorococcus* in the North Atlantic subtropical gyre. *ISME J.* 7, 603–614. doi: 10.1038/ismej.2012.126
- Gómez-Pereira, P. R., Schüler, M., Fuchs, B. M., Bennke, C., Teeling, H., Waldmann, J., et al. (2012). Genomic content of uncultured *Bacteroidetes* from contrasting oceanic provinces in the North Atlantic Ocean. *Environ. Microbiol.* 14, 52–66. doi: 10.1111/j.1462-2920.2011.02555.x
- Gonzalez, J. M., Fernandez-Gomez, B., Fernandez-Guerra, A., Gómez-Consarnau, L., Sanchez, O., Coll-Llado, M., et al. (2008). From the cover: genome analysis of the proteorhodopsin-containing marine bacterium *Polaribacter* sp. MED152 (*Flavobacteria*). *Proc. Natl. Acad. Sci. U.S.A.* 105, 8724–8729. doi: 10.1073/pnas.0712027105
- Grossart, H.-P., Tang, K. W., Kiørboe, T., and Ploug, H. (2007). Comparison of cell-specific activity between free-living and attached bacteria using isolates and natural assemblages. *FEMS Microbiol. Lett.* 266, 194–200. doi: 10.1111/j.1574-6968.2006.00520.x
- Guillard, R. R. L. (1975). “Culture of phytoplankton for feeding marine invertebrates,” in *Culture of Marine Invertebrate Animals*, eds W. L. Smith and M. H. Chanley (New York, NY: Plenum Press), 26–60.
- Guillot, L., Bachar, D., Audic, S., Bass, D., Berney, C., and Bittner, L. (2013). The protist ribosomal reference database (PR2): a catalog of unicellular eukaryote Small Sub-Unit rRNA sequences with curated taxonomy. *Nucleic Acids Res.* 41, D597–D604. doi: 10.1093/nar/gks1160
- Guindon, S., Dufayard, J. F., Lefort, V., Anisimova, M., Hordijk, W., and Gascuel, O. (2010). New algorithms and methods to estimate maximum-likelihood phylogenies: assessing the performance of phyML 3.0. *Syst. Biol.* 59, 307–321. doi: 10.1093/sysbio/syq010
- Hagström, A., Azam, F., Berg, C., and Zweifel, U. L. (2017). Isolates as models to study bacterial ecophysiology and biogeochemistry. *Aquat. Microb. Ecol.* 80, 15–27. doi: 10.3354/ame01838
- Hobbie, J. E., Daley, R. J., and Jasper, S. (1977). Use of nuclepore filters for counting bacteria by fluorescence microscopy. *Appl. Environ. Microbiol.* 33, 1225–1228.
- Inoue, K., Ono, H., Abe-Yoshizumi, R., Yoshizawa, S., Ito, H., Kogure, K., et al. (2013). A light-driven sodium ion pump in marine bacteria. *Nat. Commun.* 4:1678. doi: 10.1038/ncomms2689
- Kiørboe, T., Tang, K., Grossart, H.-P., and Ploug, H. (2003). Dynamics of microbial communities on marine snow aggregates: colonization, growth, detachment, and grazing mortality of attached bacteria. *Appl. Environ. Microbiol.* 69, 3036–3047. doi: 10.1128/AEM.69.6.3036-3047.2003
- Kirchman, D. L. (2002). The ecology of *Cytophaga-Flavobacteria* in aquatic environments. *FEMS Microbiol. Ecol.* 39, 91–100. doi: 10.1111/j.1574-6941.2002.tb00910.x
- Koblížek, M. (2015). Ecology of aerobic anoxygenic phototrophs in aquatic environments. *FEMS Microbiol. Rev.* 39, 854–870. doi: 10.1093/femsre/fuv032
- Kolber, Z. S., Van Dover, C. L., and Falkowski, P. G. (2000). Bacterial photosynthesis in surface waters of the open ocean. *Nature* 407, 177–179. doi: 10.1038/35025044
- Love, M. I., Huber, W., and Anders, S. (2014). Moderated estimation of fold change and dispersion for RNA-seq data with DESeq2. *Genome Biol.* 15:550. doi: 10.1186/s13059-014-0550-8
- Ludwig, W., Strunk, O., Westram, R., Richter, L., Meier, H., Yadhukumar, et al. (2004). ARB: a software environment for sequence data. *Nucleic Acids Res.* 32, 1363–1371. doi: 10.1093/nar/gkh293
- Maresca, J. A., Miller, K. J., Keffer, J. L., Sabanayagam, C. R., and Campbell, B. J. (2018). Distribution and diversity of rhodopsin-producing microbes in the Chesapeake Bay. *Appl. Environ. Microbiol.* 84, e137–e118. doi: 10.1128/AEM.00137-18
- Martin, M. (2011). Cutadapt removes adapter sequences from high-throughput sequencing reads. *EMBnet. J.* 17, 10–12. doi: 10.14806/embnet.17.1.200
- Mary, I., Tarran, G. A., Warwick, P. E., Terry, M. J., Scanlan, D. J., Burkill, P. H., et al. (2008). Light enhanced amino acid uptake by dominant bacterioplankton groups in surface waters of the Atlantic Ocean. *FEMS Microbiol. Ecol.* 63, 36–45. doi: 10.1111/j.1574-6941.2007.00414.x
- Mayali, X., Stewart, B., Mabery, S., and Weber, P. K. (2016). Temporal succession in carbon incorporation from macromolecules by particle-attached bacteria in marine microcosms. *Environ. Microbiol. Rep.* 8, 68–75. doi: 10.1111/1758-2229.12352
- Mayali, X., Weber, P. K., Brodie, E. L., Mabery, S., Hoepflich, P. D., and Pett-Ridge, J. (2012). High-throughput isotopic analysis of RNA microarrays to quantify microbial resource use. *ISME J.* 6, 1210–1221. doi: 10.1038/ismej.2011.175
- Mayer, L. M., Schick, L. L., Hardy, K. R., and Estapa, M. L. (2009). Photodissolution and other photochemical changes upon irradiation of algal detritus. *Limnol. Oceanogr.* 54, 1688–1698. doi: 10.4319/lo.2009.54.5.1688
- McMurdie, P. J., and Holmes, S. (2013). phyloseq: an R package for reproducible interactive analysis and graphics of microbiome census data. *PLoS One* 8:e61217. doi: 10.1371/journal.pone.0061217
- Michelou, V. K., Cottrell, M. T., and Kirchman, D. L. (2007). Light-stimulated bacterial production and amino acid assimilation by cyanobacteria and other microbes in the North Atlantic Ocean. *Appl. Environ. Microbiol.* 73, 5539–5546. doi: 10.1128/AEM.00212-07
- Milledge, J. J., and Heaven, S. (2013). A review of the harvesting of micro-algae for biofuel production. *Rev. Environ. Sci. Biol.* 12, 165–178. doi: 10.1007/s11157-012-9301-z
- Morris, J. J., Lenski, R. E., and Zinser, E. R. (2012). The black queen hypothesis: evolution of dependencies through adaptive gene loss. *mBio* 3, e36–e12. doi: 10.1128/mBio.00036-12
- Needham, D. M., Chow, C. E. T., Cram, J. A., Sachdeva, R., Parada, A., and Fuhrman, J. A. (2013). Short-term observations of marine bacterial and viral communities: patterns, connections and resilience. *ISME J.* 7, 1274–1285. doi: 10.1038/ismej.2013.19
- Needham, D. M., Fichot, E. B., Wang, E., Berdjeb, L., Cram, J. A., Fichot, C. G., et al. (2018). Dynamics and interactions of highly resolved marine plankton via automated high-frequency sampling. *ISME J.* 12, 2417–2432. doi: 10.1038/s41396-018-0169-y
- Needham, D. M., and Fuhrman, J. A. (2016). Pronounced daily succession of phytoplankton, archaea and bacteria following a spring bloom. *Nat. Microbiol.* 1:16005. doi: 10.1038/NMICROBIOL.2016.5
- Ottesen, E. A., Young, C. R., Eppley, J. M., Ryan, J. P., Chavez, F. P., Scholin, C. A., et al. (2013). Pattern and synchrony of gene expression among sympatric marine microbial populations. *Proc. Natl. Acad. Sci. U.S.A.* 110, E488–E497. doi: 10.1073/pnas.1222099110
- Ottesen, E. A., Young, C. R., Gifford, S. M., Eppley, J. M., and Marin, R. (2014). Multispecies diel transcriptional oscillations in open ocean heterotrophic bacterial assemblages. *Science* 345, 204–207. doi: 10.1126/science.1252717
- Parada, A. E., Needham, D. M., and Fuhrman, J. A. (2016). Every base matters: assessing small subunit rRNA primers for marine microbiomes with mock communities, time series and global field samples. *Environ. Microbiol.* 18, 1403–1414. doi: 10.1111/1462-2920.13023
- Passow, U., Engel, A., and Ploug, H. (2003). The role of aggregation for the dissolution of diatom frustules. *FEMS Microbiol. Ecol.* 46, 247–255. doi: 10.1016/S0168-6496(03)00199-5
- Pinhassi, J. H. J., DeLong, E. F., Beja, O., Gonzalez, J. M., and Pedrós-Alió, C. (2016). Marine bacterial and archaeal ion-pumping rhodopsins: genetic diversity. *Physiol. Ecol. Microbiol. Mol. Biol. Rev.* 80, 929–954. doi: 10.1128/MMBR.00003-16
- Ploug, H. (2001). Small-scale oxygen fluxes and remineralization in sinking aggregates. *Limnol. Oceanogr.* 46, 1624–1631. doi: 10.4319/lo.2001.46.7.1624

- Pruesse, E., Quast, C., Knittel, K., Fuchs, B. M., Ludwig, W., Peplies, J., et al. (2007). SILVA: a comprehensive online resource for quality checked and aligned ribosomal RNA sequence data compatible with ARB. *Nucleic Acids Res.* 35, 7188–7196. doi: 10.1093/nar/gkm864
- Quast, C., Pruesse, E., Yilmaz, P., Gerken, J., Schweer, T., Yarza, P., et al. (2013). The SILVA ribosomal RNA gene database project: improved data processing and web-based tools. *Nucleic Acids Res.* 41, D590–D596. doi: 10.1093/nar/gks1219
- Riedel, T., Gómez-Consarnau, L., Tomasch, J., Martin, M., Jarek, M., Gonzalez, J. M., et al. (2013). Genomics and physiology of a marine flavobacterium encoding a proteorhodopsin and a xanthorhodopsin-like protein. *PLoS One* 8:e57487. doi: 10.1371/journal.pone.0057487.s007
- Rontani, J.-F. (2001). Visible light-dependent degradation of lipidic phytoplanktonic components during senescence: a review. *Photochemistry* 58, 187–202. doi: 10.1016/s0031-9422(01)00202-3
- Ruiz-González, C., Simó, R., Sommaruga, R., and Gasol, J. M. (2013). Away from darkness: a review on the effects of solar radiation on heterotrophic bacterioplankton activity. *Front. Microbiol.* 4:131. doi: 10.3389/fmicb.2013.00131
- Sarmento, H., and Gasol, J. M. (2012). Use of phytoplankton-derived dissolved organic carbon by different types of bacterioplankton. *Environ. Microbiol.* 14, 2348–2360. doi: 10.1111/j.1462-2920.2012.02787.x
- Shanks, A. L., and Edmondson, E. W. (1989). Laboratory-made artificial marine snow - a biological model of the real thing. *Mar. Biol.* 101, 463–470. doi: 10.1007/bf00541648
- Sieradzki, E. T., Fuhrman, J. A., Rivero-Calle, S., and Gomez-Consarnau, L. (2018). Proteorhodopsins dominate the expression of phototrophic mechanisms in seasonal and dynamic marine picoplankton communities. *PeerJ* 6:e5798. doi: 10.7717/peerj.5798
- Simon, M., Grossart, H.-P., Schweitzer, B., and Ploug, H. (2002). Microbial ecology of organic aggregates in aquatic ecosystems. *Aquat. Microb. Ecol.* 28, 175–211. doi: 10.3354/ame028175
- Singh-Gasson, S., Green, R. D., Yue, Y., Nelson, C., Blattner, F., Sussman, M. R., et al. (1999). Maskless fabrication of light-directed oligonucleotide microarrays using a digital micromirror array. *Nat. Biotechnol.* 17, 974–978. doi: 10.1038/13664
- Teeling, H., Fuchs, B. M., Becher, D., Klockow, C., Gardebrecht, A., Bennke, C. M., et al. (2012). Substrate-controlled succession of marine bacterioplankton populations induced by a phytoplankton bloom. *Science* 336, 608–611. doi: 10.1126/science.1218344
- Teeling, H., Fuchs, B. M., Bann, C. M., Krueger, K., Chafee, M., Kappelmann, L., et al. (2016). Recurring patterns in bacterioplankton dynamics during coastal spring algae blooms. *eLife* 5:e11888. doi: 10.7554/eLife.11888
- Unanue, M., Azúa, I., Arrieta, J., Labirua-Iturburu, A., Egea, L., and Iriberrri, J. (1998). Bacterial colonization and ectoenzymatic activity in phytoplankton-derived model particles: cleavage of peptides and uptake of amino acids. *Microb. Ecol.* 35, 136–146. doi: 10.1007/s002489900068
- Wagner-Döbler, I., and Biebl, H. (2006). Environmental biology of the marine roseobacter lineage. *Annu. Rev. Microbiol.* 60, 255–280. doi: 10.1146/annurev.micro.60.080805.142115
- Wang, Q., Garrity, G. M., Tiedje, J. M., and Cole, J. R. (2007). Naive Bayesian classifier for rapid assignment of rRNA sequences into the new bacterial taxonomy. *Appl. Environ. Microbiol.* 73, 5261–5267. doi: 10.1128/aem.00062-07
- Williams, T. J., Wilkins, D., Long, E., Evans, F., DeMaere, M. Z., Raftery, M. J., et al. (2013). The role of planktonic Flavobacteria in processing algal organic matter in coastal East Antarctica revealed using metagenomics and metaproteomics. *Environ. Microbiol.* 15, 1302–1317. doi: 10.1111/1462-2920.12017
- Wright, E. S., Yilmaz, L. S., and Noguera, D. R. (2012). DECIPHER, a search-based approach to chimera identification for 16S rRNA sequences. *Appl. Environ. Microbiol.* 78, 717–725. doi: 10.1128/AEM.06516-11
- Yoshizawa, S., Kumagai, Y., Kim, H., Ogura, Y., Hayashi, T., Iwasaki, W., et al. (2014). Functional characterization of flavobacteria rhodopsins reveals a unique class of light-driven chloride pump in bacteria. *Proc. Natl. Acad. Sci. U.S.A.* 111, 6732–6737. doi: 10.1073/pnas.1403051111

**Conflict of Interest Statement:** The authors declare that the research was conducted in the absence of any commercial or financial relationships that could be construed as a potential conflict of interest.

Copyright © 2019 Gómez-Consarnau, Needham, Weber, Fuhrman and Mayali. This is an open-access article distributed under the terms of the Creative Commons Attribution License (CC BY). The use, distribution or reproduction in other forums is permitted, provided the original author(s) and the copyright owner(s) are credited and that the original publication in this journal is cited, in accordance with accepted academic practice. No use, distribution or reproduction is permitted which does not comply with these terms.